Autoresonance in a strongly nonlinear chain driven at one end

Agnessa Kovaleva
Space Research Institute, Russian Academy of Sciences, Moscow 117997, Russia

(Received 19 August 2018; revised manuscript received 11 October 2018; published 28 November 2018)

This work examines the emergence of autoresonance (AR) in a one-dimensional chain of strongly nonlinear oscillators subjected to a harmonic force with a slowly varying frequency applied at the end of the chain. The dynamics of the chain is studied assuming 1:1 (fundamental) resonance, when the response of each nonlinear oscillator has a dominant harmonic component with the frequency close to the frequency of the external excitation. Explicit asymptotic equations describing the amplitudes and the phases of the oscillations are derived. These equations demonstrate that, in contrast to the chain with a linear attachment, the strongly nonlinear chain can be entirely captured into resonance provided that its structural and excitation parameters exceed certain critical thresholds but the frequency detuning rate is small enough. It is shown that at large times the amplitudes of all oscillators captured into AR converge to a common monotonically growing quasisteady backbone curve. This implies asymptotic equipartition of energy between the oscillators under the condition of AR. Numerical simulations have been performed for two-, four-, and 12-particle arrays with fixed forcing and coupling parameters and different detuning rates. The obtained results demonstrate the existence of two intervals of the rate's values corresponding to AR and small-amplitude oscillations in the entire chain, respectively, and a narrow gap between these two intervals, wherein each oscillator may escape from resonance individually or in combination with neighboring particles. This implies a negligibly small interval of energy localization in a part of the chain adjacent to the source of energy compared to the interval of the emergence of AR in the entire chain.

DOI: 10.1103/PhysRevE.98.052227

I. INTRODUCTION

In this work we examine the emergence of autoresonance (AR) in a one-dimensional strongly nonlinear chain. The chain is driven by a harmonic force with a slowly varying frequency applied to the first oscillator. We recall that a large class of systems exhibits AR due to an intrinsic property of a nonlinear oscillator to change both its amplitude and natural frequency when the driving frequency changes. This means that an oscillator may remain persistently captured into resonance with its drive if the driving frequency, being initially close or equal to the natural frequency of the oscillator, varies slowly in time to be consistent with the slowly changing frequency of the oscillator. The ability of a nonlinear oscillator to stay captured into resonance due to variance of its structural or/and excitation parameters is known as *autoresonance* (AR). It is important to note that AR leads to a persistently growing mean amplitude of oscillations, and thus, this process may be employed to attain the required energy level.

After first studies in the fields of particle acceleration [1–3] and planetary dynamics [4,5], a large number of theoretical approaches, experimental results, and applications of AR in different fields of natural science have been reported in the literature (e.g., [6–8], and references therein). The derived methods and results further motivate the development of the theory and experiments for more complicated processes, such as excitations of plasma waves [9–11], particle transport in a weak external field with the slowly changing frequency [12,13], energy conversion [14], control of nanoparticles [15], etc.

Since there are a small number of nonlinear equations for which analytic solutions are available, most of the above-mentioned results have been obtained with the help of numerical or/and experimental modeling. In most of these studies, AR in the forced oscillator was considered as an effective tool for exciting high-energy oscillations in the entire system. However, recent results [16–19] have shown that this principle is not universal because capture into resonance of a multiparticle chain is a much more complicated phenomenon than a similar effect for a single oscillator, and the emergence of AR in coupled oscillators directly depends on the structure of the chain. The occurrence of AR in quasilinear Klein-Gordon chains was investigated analytically and numerically in recent works [18,19]. The purpose of this work is to investigate the emergence of AR in a multiparticle strongly nonlinear chain driven by a periodic force with slowly varying frequency applied at one end of the chain. This study is motivated by the results earlier obtained for a resonant anharmonic chain driven by a periodic force with a constant frequency [20].

Although an anharmonic oscillator does not possess a natural frequency independent of the energy of the oscillations, the most effective energy transport in the nonlinear chain occurs due to 1:1 (fundamental) resonance, when the response of the chain is approximately monochromatic with the frequency close to the excitation frequency (see, e.g., [21]). This assumption allows the reduction of the original nonlinear equations to the formally quasilinear system, with further applications of the well-developed multiple-scale and averaging procedures [22,23]. In this work, a similar approach is extended to the analysis of AR in the chain driven by a harmonic force with a slowly varying frequency.

Section II introduces the equations of the chain dynamics. The small parameter of the system is defined as the dimensionless coupling strength. Rearranging the equations of motion to the form convenient for the analysis of 1:1 resonance and applying the multiple timescale formalism, we obtain the averaged equations for the slowly varying amplitudes and phases of resonant oscillations. Then we calculate the quasisteady amplitudes, which can be interpreted as the backbone curves of oscillators. Both analytical and numerical simulations show that the quasisteady amplitudes converge to a slowly increasing smooth backbone curve common for all oscillators, and amplitudes of all particles fluctuate about this curve. This effect demonstrates asymptotic equipartition of energy between all oscillators under the condition of AR.

In Sec. III the derived averaged equations are used to determine the parametric domain, in which stable AR may occur. Note that not only admissible coupling parameters and forcing amplitudes but also the critical detuning rate is estimated for a basic single oscillator. Examples of a single oscillator and a pair of coupled oscillators [16,24] have demonstrated that the critical detuning rate requires additional numerical verification.

Numerical results in Sec. IV have been obtained for two-, four-, and 12-particle arrays with admissible fixed coupling and forcing parameters and different detuning rates. Numerical results demonstrate the existence of two intervals of the rate's values corresponding to AR and small-amplitude oscillations in the entire chain, respectively. The width of a gap between these two intervals, in which each oscillator may escape from resonance individually or in combination with neighboring particles, is on the order of 0.1% of the length of the first interval. Concluding remarks are collected together in the last section.

II. MODEL

We examine the emergence of autoresonance (AR) in a one-dimensional chain consisting of n identical weakly linearly coupled cubic oscillators. The chain is driven by a harmonic force with a slowly varying frequency applied to the first oscillator. The chain dynamics is governed by the equations

$$\begin{aligned}&\frac{d^2U_r}{dt^2}+\gamma U_r^3+k[\eta_{r,r-1}(U_r-U_{r-1})\\&\quad+\eta_{r,r+1}(U_r-U_{r+1})]=A_r\sin\theta,\\&\frac{d\theta}{dt}=\omega+\zeta(t);\quad \zeta(t)=kt,\end{aligned}\tag{1}$$

where U_r denotes the absolute displacement of the rth oscillator from its rest state, $r\in[1,n]$; γ is the cubic stiffness coefficient; κ is the coefficient of linear coupling; all parameters are reduced to unit mass. The coefficients $\eta_{r,l}=\{1, l\in[1,n];\ 0, l=0, l=n+1\}$ indicate that the edge oscillators are unilaterally coupled with the adjacent elements. Since the harmonic excitation is applied only to the first oscillator, we let $A_1=A$, $A_r=0$ at $r\geqslant 2$. The chain is assumed to be initially at rest; i.e., $U_r=0$, $V_r=dU_r/dt=0$ at $t=0$ for all oscillators. Recall that the initial rest state determines the so-called *limiting phase trajectory* (LPT) [25] corresponding to maximum possible energy transfer from the source of energy to the excited oscillator.

For further analysis, it is convenient to reduce (1) to the dimensionless form, which has a simpler structure than (1). Assuming weak coupling, we introduce the small parameter of the system $\varepsilon=\kappa/(2\omega^2)\ll 1$, where $\kappa/\omega^2=2\varepsilon$ is the dimensionless coupling strength. The dimensionless variables are defined as $u_r=\alpha^{1/2}U_r$, where $\alpha=3\gamma/4\omega^2$; the dimensionless fast and slow timescales are given by $\tau_0=\omega t$ and $\tau=\varepsilon\tau_0$, respectively. The forcing amplitude f and detuning rate β are defined by formulas $2\varepsilon f=\alpha^{1/2}A/\omega^2$, $\varepsilon^2\beta=k/\omega^2$. Substituting the new variables and parameters into (1), we obtain the following dimensionless equations:

$$\begin{aligned}&\frac{d^2u_r}{d\tau_0^2}+\frac{4}{3}u_r^3+2\varepsilon[\eta_{r,r-1}(u_r-u_{r-1})+\eta_{r,r+1}(u_r-u_{r+1})]\\&\quad=2\varepsilon f_r\sin\theta,\quad \frac{d\theta}{d\tau_0}=1+\varepsilon\zeta_0(\tau),\ \zeta_0(\tau)=\beta\tau,\end{aligned}\tag{2}$$

where the amplitude f_r of the driving force is nonzero only at $r=1$ but $f_r=0$ at $r\in[2,n]$. Although the generating nonlinear system $\frac{d^2u_r}{d\tau_0^2}+\frac{4}{3}u_r^3=0$ does not possess a spectrum independent of the energy of the oscillations, intense energy transport in (2) is studied under the assumption of 1:1 (fundamental) resonance, i.e., under the condition that the response of each oscillator in the chain has a dominant harmonic component with the frequency close to the excitation frequency. Under this assumption, the equations of resonant oscillations are rewritten as

$$\begin{aligned}&\frac{d^2u_r}{d\tau_0^2}+u_r+2\varepsilon\bigg[\sigma\left(\frac{4}{3}u_r^3-u_r\right)+\eta_{r,r-1}(u_r-u_{r-1})\\&\quad+\eta_{r,r+1}(u_r-u_{r+1})\bigg]=2\varepsilon f_r\sin\theta,\quad \frac{d\theta}{d\tau_0}=1+\varepsilon\zeta_0(\tau),\end{aligned}\tag{3}$$

where $2\varepsilon\sigma=1$. Since the equations in system (3) are formally quasilinear, the earlier developed methods [18,19] can be applied to the study of the resonant behavior of the anharmonic chain. To this end, the following complex-valued envelopes are introduced:

$$\psi_r=\left(\frac{du_r}{d\tau_0}+iu_r\right)e^{-i\theta},\quad \psi_r^*=\left(\frac{du_r}{d\tau_0}-iu_r\right)e^{i\theta}.\tag{4}$$

It follows from (4) that the real-valued dimensionless amplitudes and phases of oscillations are expressed as $\tilde{a}_r=|\psi_r|$ and $\widetilde{\Delta}_r=\arg\psi_r$, respectively. Substituting (4) into (3), we derive the following (still exact) equations for the envelopes ψ_r:

$$\begin{aligned}\frac{\mathrm{d}\psi_r}{\mathrm{d}\tau_0}&=i\varepsilon[\sigma(|\psi_r|^2-1)\psi_r-\zeta_0(\tau)\psi_r+\eta_{r,r-1}(\psi_r-\psi_{r-1})\\&\quad+\eta_{r,r+1}(\psi_r-\psi_{r+1})-f_r+G_r]\end{aligned}\tag{5}$$

and similar equations for the complex-conjugate variables ψ_r^*, $r\in[1,n]$. The system is initially at rest, that is, $\psi_r(0)=\psi_r^*(0)=0$. The coefficients G_r include higher harmonics in θ with coefficients depending on the components of the fast vectors ψ and ψ^*. As shown in [18,19], explicit expressions of these coefficients are insignificant for further analysis.

The multiple timescale approach [22] is employed to construct asymptotic approximations to the solutions of (5). To this end, the following asymptotic decomposition is introduced:

$$\psi_r(\tau_0,\tau,\varepsilon)=\psi_r^{(0)}(\tau)+\varepsilon\psi_r^{(1)}(\tau_0,\tau)+O(\varepsilon^2). \quad (6)$$

The straightforward averaging of (5) with respect to the fast time τ_0 yields the following equations for the leading-order slow terms $\psi_r^{(0)}(\tau)$:

$$\frac{d\psi_r^{(0)}}{d\tau}=i\big[\sigma\big(\big|\psi_r^{(0)}\big|^2-1\big)\psi_r^{(0)}-\zeta_0(\tau)\psi_r^{(0)} +\eta_{r,r-1}\big(\psi_r^{(0)}-\psi_{r-1}^{(0)}\big)+\eta_{r,r+1}\big(\psi_r^{(0)}-\psi_{r+1}^{(0)}\big)-f_r\big] \quad (7)$$

and similar equations for the complex-conjugate variables. Note that, in contrast to Eq. (5), the averaged equations do not contain the periodic in θ coefficients, and the solution of system (7) represents the slowly varying vector function $\psi^{(0)}(\tau)$ with components $\psi_r^{(0)}(\tau)$.

Finally, the change of variables,

$$\psi_r^{(0)}=a_re^{i\Delta_r},\quad a_r=\big|\psi_r^{(0)}\big|,\quad \Delta_r=\arg\psi_r^{(0)}, \quad (8)$$

transforms (7) into the following equations:

$$\begin{aligned}\frac{da_r}{d\tau}&=[\eta_{r,r-1}a_{r-1}\sin(\Delta_{r-1}-\Delta_r)\\&\quad+\eta_{r,r+1}a_{r+1}\sin(\Delta_{r+1}-\Delta_r)]-f_r\sin\Delta_r,\\ a_r\frac{d\Delta_r}{d\tau}&=\sigma\big(a_r^2-1\big)a_r-\zeta_0(\tau)a_r\\&\quad+\{\eta_{r,r-1}[a_r-a_{r-1}\cos(\Delta_{r-1}-\Delta_r)]\\&\quad+\eta_{r,r+1}[a_r-a_{r+1}\cos(\Delta_{r+1}-\Delta_r)]\}-f_r\cos\Delta_r,\end{aligned} \quad (9)$$

with initial amplitudes $a_r(0)=0$ and uncertain initial phases $\Delta_r(0)$, $r\in[1,n]$. To overcome this uncertainty, one needs to solve the nonsingular complex-valued equations in system (7) with fixed initial conditions and then calculate the real-valued amplitudes and phases by the formulas in Eq. (8).

Numerical results presented below have been obtained from the regular equations in (7). We note that Eqs. (7) and (9) at $\zeta_0(\tau)=0$ coincide with similar equations for the slow envelopes in the system driven by a harmonic excitation with a constant frequency [20].

It was recently demonstrated [18,19] that the AR amplitudes in the quasilinear chain can be depicted as the superposition of fast oscillations on the adiabatically varying backbone curves. We show that this result remains valid for the anharmonic system. The quasisteady solutions $\bar{a}_r$, $\bar{\Delta}_r$ of (9) satisfy the equations

$$P_r=\frac{da_r}{d\tau}=0,\quad Q_r=\frac{d\Delta_r}{d\tau}=0,\quad r\in[1,n]. \quad (10)$$

The equality $P_n=0$ implies that $\sin(\Delta_n-\Delta_{n-1})=0$. Substituting the latter equality into the condition $P_{n-1}=0$ we then have $\sin(\Delta_{n-1}-\Delta_{n-2})=0$. Repeating this procedure for each equation $P_r=0$, we obtain $\sin(\Delta_r-\Delta_{r-1})=0$, $\sin\Delta_1=0$. This means that either $\overline{\Delta}_r=0\pmod{2\pi}$ or $\overline{\Delta}_r=-\pi\pmod{2\pi}$, $r\in[1,n]$. The analysis of the variational equations linearized near $\bar{a}_r$, $\overline{\Delta}_r$ proves that, in analogy to a single oscillator, the phases $\overline{\Delta}_r=0\pmod{2\pi}$ correspond to the stable AR. Quasisteady amplitudes $\bar{a}_r$ corresponding to AR in the entire chain are defined by the following equations:

$$\begin{aligned}&\sigma\big(a_1^2-1\big)a_1-\zeta_0(\tau)a_1+(a_1-a_2)-f=0,\\&\sigma\big(a_r^2-1\big)a_r-\zeta_0(\tau)a_r+(2a_r-a_{r-1}-a_{r+1})=0,\\&r\in[2,n-1],\\&\sigma\big(a_n^2-1\big)a_n-\zeta_0(\tau)a_n+(a_n-a_{n-1})=0,\end{aligned} \quad (11)$$

with the solutions

$$\begin{aligned}\bar{a}_1(\tau)&=\rho_\varepsilon(\tau)+\varepsilon\left(\frac{f}{\rho_\varepsilon^2(\tau)}\right)+\varepsilon^2O\left[\frac{f}{\rho_\varepsilon^5(\tau)}\right],\\ \bar{a}_r(\tau)&=\rho_\varepsilon(\tau)+\varepsilon^rO\left[\frac{f}{\rho_\varepsilon^{2r}(\tau)}\right],\quad r\in[2,n-1],\end{aligned} \quad (12)$$

where the leading-order term $\rho_\varepsilon(\tau)=[1+2\varepsilon\zeta_0(\tau)]^{1/2}$ approximates the backbone curve identical for all oscillators. Since $\rho_\varepsilon(\tau)\to\infty$ as $\tau\to\infty$, it follows from (12) that the higher-order corrections may be ignored, and $\bar{a}_r(\tau)\to\rho_\varepsilon(\tau)$ at large times (see Fig. 2). This implies that energy initially placed in the first oscillator approaches equipartition among all particles at large times. This conclusion is illustrated below by the results of numerical simulations.

III. CRITICAL PARAMETERS

In this section we demonstrate that, in contrast to the array with a linear attachment [17], a proper choice of the structural and excitation parameters guarantees the emergence of AR in the anharmonic chain. Since the coupling response acts as an external excitation with respect to the attachment, the emergence of AR in the forced oscillator can be considered as a necessary condition of capture into resonance of the entire chain. This means that the threshold values of the parameters ε and f can be found assuming small oscillations of the attachment. This means that the problem can be reduced to the analysis of (7) under the conditions $|\psi_1|\sim O(1)$ but $|\psi_r|\sim o(1)$, $r\in[2,n]$. Under this assumption, the equations of the excited oscillator are approximated as follows:

$$\begin{aligned}\frac{da_1}{d\tau}&=-f\sin\Delta_1,\\ a_1\frac{d\Delta_1}{d\tau}&=\sigma\big(a_1^2-1\big)a_1-\zeta_0(\tau)a_1+a_1-f\cos\Delta_1.\end{aligned} \quad (13)$$

It was shown in earlier work [24] that the envelope $a_1(\tau)$ for sufficiently small τ is very close to the LPT of a similar time-independent system with $\zeta_0(\tau)=0$. Thus the first step towards analyzing AR is the study of the transition from small to large oscillations in the underlying system with a constant excitation frequency. The equations of the excited oscillator at $\zeta_0=0$ are given by

$$\begin{aligned}\frac{da_1}{d\tau}&=-f\sin\Delta_1,\\ a_1\frac{d\Delta_1}{d\tau}&=\sigma\big(a_1^2-1\big)a_1+a_1-f\cos\Delta_1,\end{aligned} \quad (14)$$

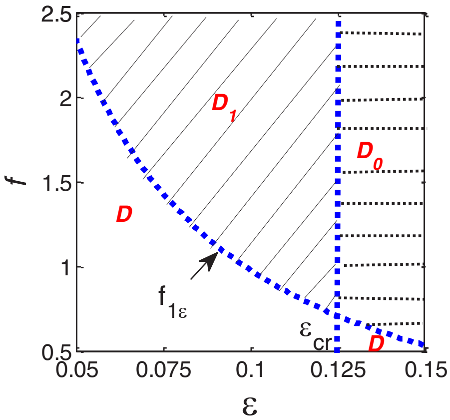

FIG. 1. Parametric boundaries (15) and (16): all particles with parameters $(\varepsilon, f) \in D$ execute small oscillations; the entire chain with parameters $(\varepsilon, f) \in D_0$ is captured into resonance; if $(\varepsilon, f) \in D_1$, then the forced oscillator is captured into resonance but the dynamics of the attachment should be investigated separately.

with initial condition $a_1(0) = 0$, $\Delta = -\pi/2$ corresponding to the LPT of the oscillator (14). Note that the truncated model, which ignores the effect of the entire attachment including the connection with the second oscillator, was investigated in [26]. Equation (14) gives a more adequate approximation for the resonant dynamics of the excited oscillator regarding the effect of the attachment.

It was shown [25] that the transition from small to large oscillations in the system being initially at rest occurs due to the loss of stability of the LPT of small oscillations at a critical value $f = f_{1\varepsilon}$ of the forcing amplitude. The domain of large oscillations is defined as

$$f > f_{1\varepsilon} = \sqrt{(1-2\varepsilon)^3/54\varepsilon^2}. \tag{15}$$

[Inequality (15) is derived in the Appendix.] It is clearly seen that the threshold $f_{1\varepsilon}$ decreases with increasing values of the parameter ε.

The next step is to define the admissible values of the parameter ε, which yield the coupling response sufficient to sustain resonance in the rth oscillator under the condition of resonance in the previous oscillator and small oscillations of the subsequent oscillator. Reproducing the arguments from [20], we derive the constraint,

$$\varepsilon > \varepsilon_{cr} = 0.125. \tag{16}$$

Conditions (15) and (16) are presented in Fig. 1. It was recently shown [20] that the particles with parameters $(e, f) \in D$ perform small oscillations; the entire chain with parameters $(e, f) \in D_0$ is captured into resonance. If $(e, f) \in D_1$, then the forced oscillator is captured into resonance but the dynamics of the attachment should be investigated separately. Recall that conditions (15) and (16) adequately describe a parametric boundary between small and large oscillations in the system with constant excitation frequency [20]. In this paper, we show that these results cannot be directly extended to the arrays with a slowly varying excitation frequency, whose dynamics depends on the detuning rate β.

The emergence of AR also depends on the critical detuning rate β^*, at which the transition from bounded to unbounded oscillations takes place. The response amplitudes of oscillators (13) and (14) with parameters $(\varepsilon = 0.13 > \varepsilon_{cr},\ f = 0.7) \in D_0$ and different detuning rates β are presented in Fig. 2. For comparison, Fig. 2 also depicts the response amplitude of the time-invariant oscillator with the "frozen" detuning:

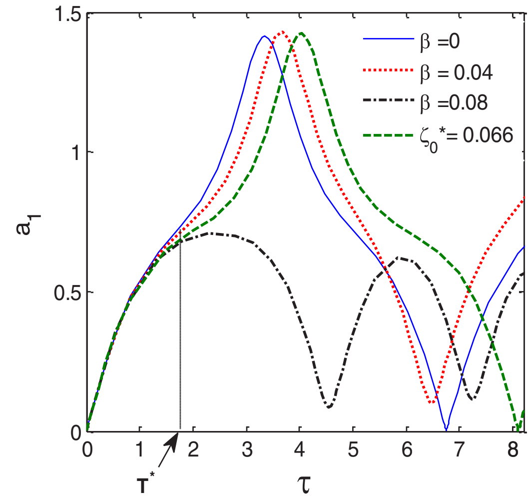

FIG. 2. Response amplitudes of oscillators (13), (14), and (17) with parameters $(\varepsilon = 0.13, f = 0.7) \in D_0$ and different detuning rates β. The inflection point $T^* \approx 1.65$ for the LPT of oscillator (14) (solid line) is close to the inflection point for the adiabatic system (13) at $\beta = 0.04$ (dotted line).

$$\frac{da_1}{d\tau} = -f \sin \Delta_1,$$

$$a_1 \frac{d\Delta_1}{d\tau} = \sigma\left(a_1^2 - 1\right)a_1 - \zeta_0^*\, a_1 + a_1 - f \cos \Delta_1, \tag{17}$$

with the constant parameter $\zeta_0^* = \beta T^*$, where T^* is an instant of inflection for the LPT of the basic oscillator (14) (Fig. 2). It is seen in Fig. 2 that the LPT of oscillator (14) has a noticeable inflection at $\tau = T^*$, and the transitions from small to large oscillations in the adiabatic system (13) also take place at $\tau \approx T^*$, despite the significant divergence of the solutions at $\tau > T^*$.

From Fig. 2, it is seen that the response amplitude of the examined oscillator (13) (dotted line) lies between the LPTs of the time-invariant oscillators (14) (solid line) and (17) (dashed line). This implies that capture into resonance of the model (17) with the frozen detuning may be considered as a sufficient condition of the emergence of AR in the original system (13). Considering $\zeta_0(T^*) = \beta T^*$ as a frozen parameter and using the results from [25], we obtain the following condition of the emergence of AR in the adiabatic oscillator:

$$2\varepsilon\beta T^* < (1-2\varepsilon)[(f/f_{1\varepsilon})^{2/3} - 1]. \tag{18}$$

It follows from (18) that the critical detuning rate β^* is given by

$$\beta^* = (1-2\varepsilon)[(f/f_{1\varepsilon})^{2/3} - 1]/(2\varepsilon T^*). \tag{19}$$

The condition $\beta < \beta^*$ admits the emergence of AR in the oscillator (13). An analytical estimate of the inflection time T^* may be obtained in the same way as in [25].

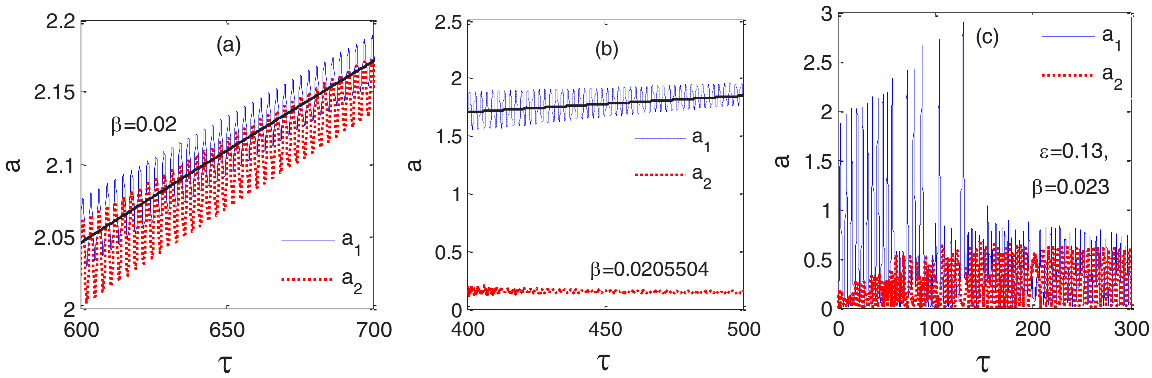

FIG. 3. Emergence of AR and escape from resonance for a pair of coupled oscillators with parameters ($\varepsilon = 0.13$, $f = 0.7$) $\in D_0$ and different detuning rate: (a) stable in-phase AR in the entire array at $\beta = 0.02$; (b) AR in the excited oscillator and escape from resonance of the attached oscillator at $\beta = 0.020\,550\,4$; (c) small-amplitude oscillations of both oscillators at $\beta = 0.023$. Bold solid lines in plots (a,b) depict the backbone curves.

Formulas (15), (18), and (19) are derived in the Appendix. In particular, it is shown that $d\beta^*/d\varepsilon\ > 0$ if $\varepsilon < 1/(\sqrt{2}f)$. This means that the critical rate β^* increases with increasing coupling strength for sufficiently small values of ε. An example is discussed in the Appendix.

Recall that the examination of AR in a single oscillator and a pair of coupled oscillators [16,24] has shown that the critical detuning rate requires additional numerical verification. To improve the correctness of numerical results for multiparticle arrays, in practical problems it is convenient to

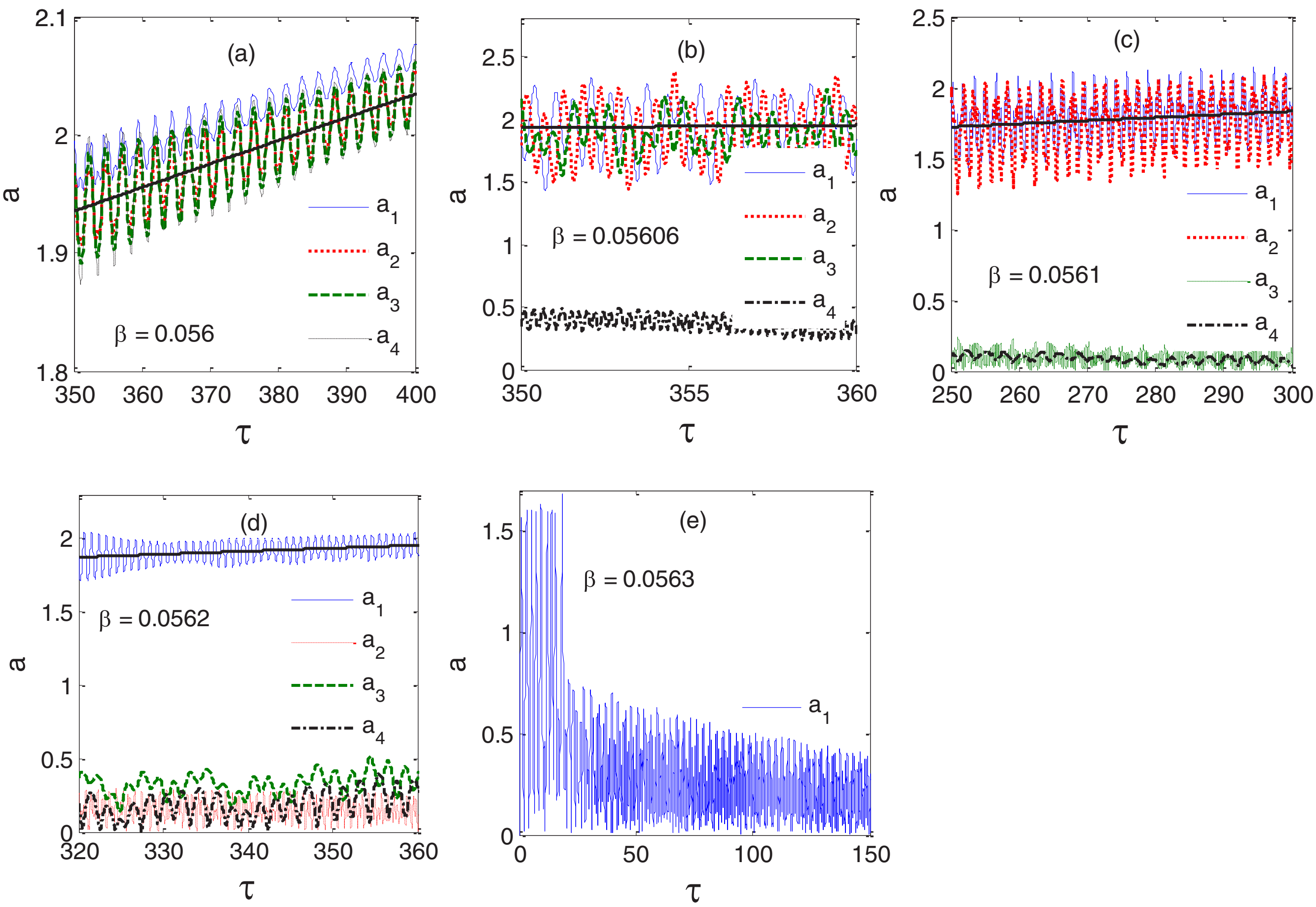

FIG. 4. Emergence of AR and escape from resonance in the four-particle chain with parameters ($\varepsilon = 0.07$, $f = 2$) $\in D_1$: (a) AR in the entire chain at $\beta = 0.056$; (b) escape from resonance of the fourth oscillator at $\beta = 0.056\,06$; (c) escape from resonance of the last two oscillators at $\beta = 0.0561$; (d) AR in the excited oscillator and escape from AR of the three-particle attachment at $\beta = 0.0562$; (e) nonresonant oscillations in the entire chain at $\beta = 0.0563$. Bold solid lines in plots (a–d) denote the segments of the backbone curves.

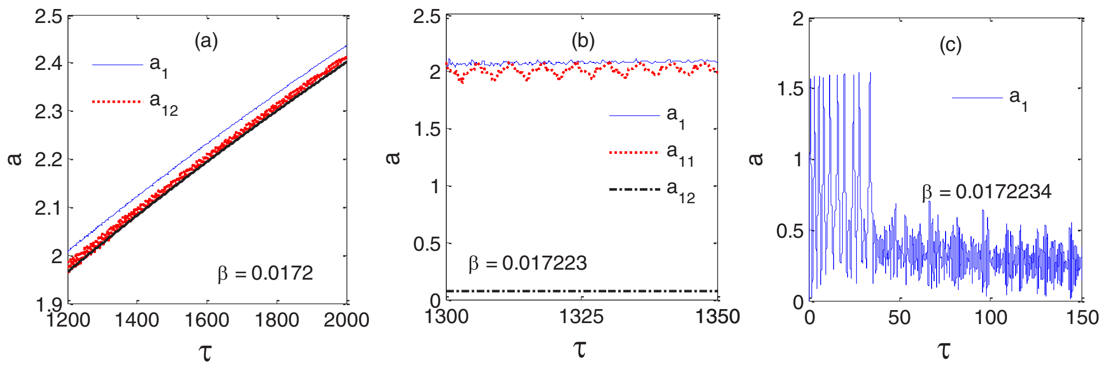

FIG. 5. Emergence of AR and escape from resonance in the 12-particle chains with parameters ($\varepsilon = 0.07$, $f = 2$) $\in D_1$ and different detuning rate: (a) AR in the entire chain at $\beta = 0.0172$; (b) escape from resonance of the last oscillator at $\beta = 0.017\,223$; (c) nonresonant oscillations in the entire chain at $\beta = 0.017\,223\,4$. Bold solid line in plot (a) depicts the backbone curve.

employ the numerically found values of the parameters T^* and β^*.

IV. NUMERICAL RESULTS

In this section we present numerical results that help us understand the influence of the detuning rate on the formation and sustenance of AR.

A. Two-particle arrays

For brevity, the influence of parameters on the resonant behavior is studied in detail only for a two-particle chain with parameter $\varepsilon = 0.13$, $f = 0.7$, and different detuning rates. It is easy to check that the parameters $(\varepsilon, f) \in D_0$, and a similar chain at $\beta = 0$ is captured into resonance. The emergence of AR and escape from resonance for the pair of coupled oscillators with parameters ($\varepsilon = 0.13$, $f = 0.7$) $\in D_0$ and different detuning is illustrated in Fig. 3.

Numerical simulation illustrates the three types of steady responses: in-phase AR in both oscillators at $\beta = 0.2$; escape from resonance of the passive attachment at $\beta = 0.205\,504$; small-amplitude oscillations of both particles at $\beta = 0.23$.

B. Four-particle arrays

Figure 4 illustrates the influence of detuning on the dynamical behavior of the four-particle chain with parameters ($\varepsilon = 0.07$, $f = 2$) $\in D_1$. Figure 4(a) demonstrates stable AR at small detuning rate; further increase of rate β leads to the sequential escape from AR of every oscillator in the chain [Figs. 4(b)–4(e)]. For clarity, the initial interval of irregular motion is shown only in Fig. 4(e). For the same purpose, the development of AR and escape from AR are illustrated in relatively short time intervals, wherein slow variations of the amplitudes are poorly pronounced but the shape of the amplitudes and the tendency to in-phase oscillations become clear. It is important to note that AR emerges in the entire chain at any rate $\beta \leqslant 0.056$ but it fails rapidly after the rate has exceeded a critical threshold.

C. Twelve-particle arrays

Figure 5 illustrates the behavior of the 12-particle chain with parameters ($\varepsilon = 0.07$, $f = 2$) $\in D_1$ and different detuning rates. For clarity, Figs. 5(a) and 5(b) depict only the amplitudes of the first and last of the oscillators captured into resonance. As in the previous example, the initial interval of irregular motion is shown only for small oscillations in Fig. 5(c). Note that AR emerges in the entire chain at any rate $\beta \leqslant 0.0172$ but all oscillators escape from resonance at $\beta \geqslant 0.017\,223\,4$. Escape from resonance of each oscillator individually or in combination with neighboring particles is defined by a greater number of decimal places (cf. Figs. 3 and 4).

Figures 3–5 demonstrate a narrow gap between the rate values which enable either AR or small-amplitude oscillations in the entire chain. This implies that the interval of the rates corresponding to escape from resonance of an individual oscillator is small compared to the interval of energy equipartition in the entire chain, and energy localization cannot be considered as a dominant factor in the chain dynamics.

V. CONCLUSIONS

In this work, we investigate the emergence and stability of autoresonance in a strongly nonlinear chain driven at one end. The chain comprises n identical weakly linearly coupled cubic oscillators; an external harmonic force with a slowly increasing frequency is applied to the first oscillator. The dynamics of the chain is studied under the assumption of 1:1 (fundamental) resonance, i.e., under the condition that the response of each nonlinear oscillator has a dominant harmonic component with a frequency close to the excitation frequency. This implies that the strongly nonlinear resonant system allows an approximate single-frequency solution with slowly varying amplitudes and phases. The equations for the slow variables have been obtained with the help of the multiple-scale and averaging procedures.

Since the coupling response acts as an external excitation with respect to the attachment, the emergence of AR in the forced oscillator can be considered as a necessary condition of capture into resonance of the entire chain. On the other hand, the coupling strength should be sufficient to sustain resonance in a chosen oscillator under the conditions of resonance in the previous oscillator. The approximate solution has demonstrated that the strongly nonlinear chain can be entirely captured into resonance provided that its structural and excitation parameters exceed certain critical thresholds. Furthermore, the amplitudes of all resonant oscillators converge to a common monotonically growing quasisteady backbone curve at large times, thus demonstrating asymptotic equipartition of energy between the resonant oscillators. If both forcing and coupling parameters are beyond the admissible domain, all particles in the chain perform small-amplitude oscillations. In the intermediate case, when only the coupling strength is below the critical value, the forced oscillator remains captured into resonance but the dynamics of the attachment should be investigated separately. Note that these effects are observed only in the array with adiabatically varying forcing frequency. Numerical simulations reveal two intervals of the rate's values corresponding to either AR or small-amplitude oscillations in the entire chain. In a narrow gap between these two intervals each oscillator may escape from resonance individually or in combination with neighboring particles.

ACKNOWLEDGMENT

Support for this work obtained from the Russian Foundation for Basic Research, 16-02-00400, 17-01-00582 is gratefully acknowledged.

APPENDIX

In this Appendix, we derive conditions (15) and (19). It can be easily verified that Eq. (17) subjected to the initial condition $a_1(0) = 0$ possesses the integral of motion

$$H = a_1\left(\sigma a_1^3 - \frac{s}{2}a_1 - f\cos\Delta_1\right) = 0, \tag{A1}$$

where $s = \sigma - 1 + \zeta_0^*$. Equality (A1) determines the LPT of system (17) on the phase plane (Δ_1, a_1). Besides, Eq. (A1) demonstrates the existence of the two branches of the LPT: The first branch is $a_1 \equiv 0$; the second branch $a_1(\Delta_1)$ satisfies the cubic equation

$$\sigma a_1^3 - \frac{s}{2}a_1 - f\cos\Delta_1 = 0. \tag{A2}$$

It follows from (A2) that $\cos\Delta_1(0) = 0$ at $a_1(0) = 0$. Assuming $\mathrm{d}a_1/d\tau > 0$ at $\tau = 0$ we obtain the initial phase of the LPT as $\Delta_1(0) = -\pi/2$ at $a_1(0) = 0$.

It follows from the condition of stationarity, $da_1/d\tau = 0$, that the steady phase $\bar{\Delta}_1$ satisfies the equation $\sin\overline{\Delta}_1 = 0$; that is, $\bar{\Delta}_1 =\ 0$ or $\overline{\Delta}_1 = -\pi$. It was shown in earlier work [25] that there exists a parametric threshold $f = f_1^*$ such that at $f < f_1^*$ the LPT represents an outer boundary for a set of small-amplitude trajectories encircling the stable center on the axis $\Delta_1 = -\pi$, while at $f > f_1^*$ the LPT depicts an outer boundary for large-amplitude trajectories encircling the stable center on the axis $\Delta_1 = 0$ (Fig. 6). The threshold f_1^* is determined through the properties of the discriminant D corresponding to Eq. (A2) at $\Delta = 0$ [27]:

$$D = \frac{36}{\sigma^2}\left(f^2 - \frac{2s^3}{27\sigma}\right). \tag{A3}$$

If $D < 0$, Eq. (A2) has three different real roots; if $D > 0$, Eq. (A2) has a single real and two complex-conjugate roots; if $D = 0$, two real roots merge [27]. The latter condition yields the critical value of the forcing amplitude f:

$$f_1^* = (2s^3/27\sigma)^{1/2} \tag{A4}$$

(cf. [25]). If the amplitude f is fixed, condition $D = 0$ determines the critical value of the parameter s:

$$s^* = 3(\sigma f^2/2)^{1/3}. \tag{A5}$$

The system exhibits small-amplitude oscillations at $s > s^*$ and large-amplitude resonant oscillations at $s < s^*$. Substituting the expressions $s = \sigma + \zeta_0^* - 1$, $\sigma = 1/2\varepsilon$, $\zeta_0^* = \beta T^*$ into (A4) and (A5), we obtain the following critical parameters:

$$f_{1\varepsilon} = \sqrt{(1-2\varepsilon)^3/54\varepsilon^2} \text{ at } \beta = 0 \tag{A6}$$

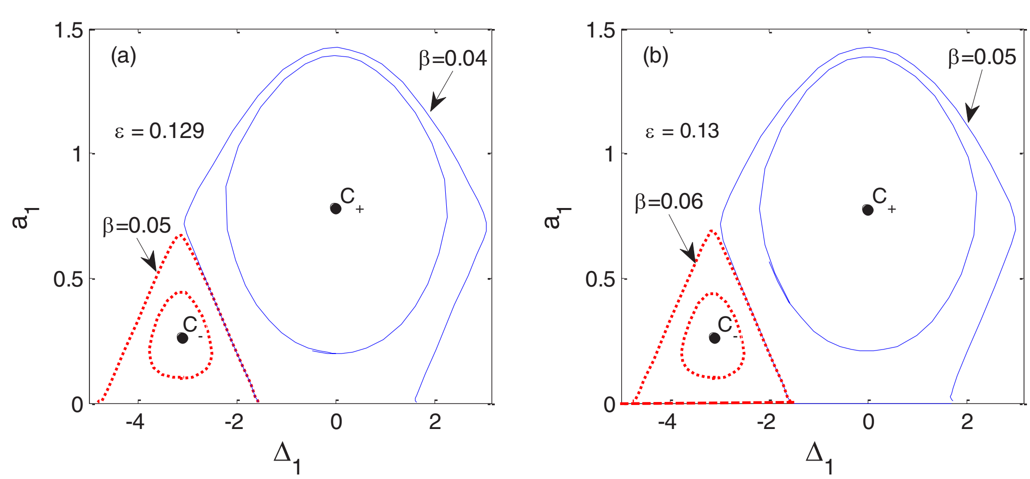

FIG. 6. Phase plots of oscillator (17): (a) $f = 0.7$, $T^* = 1.65$, $\varepsilon = 0.129$; (b) $f = 0.7$, $T^* = 1.65$, $\varepsilon = 0.13$. The encircling curves starting at $a_1 = 0$ depict the LPTs. The stable centers on the axes $\Delta_1 = 0$ and $\Delta_1 = -\pi$ are denoted as C_+ and C_-, respectively. At $\beta = 0.05$, the oscillator performs small oscillations at $\varepsilon = 0.129$ and large oscillations at $\varepsilon = 0.13$.

and

$$\beta^* = (1 - 2\varepsilon)[(f/f_{1\varepsilon})^{2/3} - 1]/(2\varepsilon T^*), \quad \beta \neq 0. \tag{A7}$$

It was indicated in Sec. III that the condition $f > f_{1\varepsilon}$ determines the domain of large oscillations for the time-invariant oscillator (14), while the condition $\beta < \beta^*$ admits the emergence of AR in the adiabatically varying system (13).

It follows from (A5) and (A7) that $d\zeta_0^*/d\varepsilon = 2\varepsilon^2[1 - (2\varepsilon^2 f^2)^{1/3}]$, $d\zeta_0^*/d\varepsilon > 0$ at $2\varepsilon^2 f^2 < 1$. This implies that the critical detuning rate β^* increases with an increase of the coupling parameter ε provided that ε is small enough.

The numerical results depicted in Fig. 6 indicate that the shape of the LPT in the frozen model (17) slightly depends on β but the critical value β^* is very sensitive to the change of the coupling parameter ε. Figure 6 demonstrates the phase plots of oscillators (17) with parameters $\varepsilon = 0.13$, $f = 0.7$ [plot (a)] and $\varepsilon = 0.129$, $f = 0.7$ [plot (b)]. The encircling curves starting at $a_1 = 0$ depict the LPTs. Formula (A5) determines the following critical parameters: $\beta^* = 0.044$ at $\varepsilon = 0.129$, $\beta^* = 0.058$ at $\varepsilon = 0.13$. In both cases, the systems exhibit small-amplitude oscillations at $\beta > \beta^*$ and large-amplitude resonance at $\beta < \beta^*$ (Fig. 6). For example, at $\beta = 0.05$ the oscillator performs small-amplitude oscillations at $\varepsilon = 0.129$ [Fig. 6(a)] and large-amplitude oscillations at $\varepsilon = 0.13$ [Fig. 6(b)].

[1] V. I. Veksler, Comptes Rendus (Doklady) de l'Académie des Sciences de l'URSS **43**, 329 (1944).
[2] E. M. McMillan, Phys. Rev. **68**, 144 (1945).
[3] M. S. Livingstone, *High Energy Accelerators* (Interscience, New York, 1954).
[4] A. T. Sinclair, Mon. Not. R. Astron. Soc. **160**, 169 (1972).
[5] R. J. Greenberg, Astron. J. **78**, 338 (1973).
[6] L. Vazquez, R. MacKay, and M. P. Zorzano, *Localization and Energy Transfer in Nonlinear Systems* (World Scientific, Singapore, 2003).
[7] V. May and O. Kühn, *Charge and Energy Transfer Dynamics in Molecular Systems* (Wiley-VCH, Weinheim, Germany, 2011).
[8] S. Rajasekar and M. A. F. Sanjuan, *Nonlinear Resonances* (Springer, Berlin, 2016).
[9] K. Gomberoff, H. Higaki, C. Kaga, K. Ito, and H. Okamoto, Phys. Rev. E **94**, 043204 (2016).
[10] I. Barth, I. Y. Dodin, and N. J. Fisch, Phys. Rev. Lett. **115**, 075001 (2015).
[11] C. J. Baker, J. R. Danielson, N. C. Hurst, and C. M. Surko, Phys. Plasmas **22**, 022302 (2015).
[12] L. M. Zelenyi, A. I. Neishtadt, A. V. Artemyev, D. L. Vainchtein, and H. V. Malova, Phys.-Usp. **56**, 347 (2013).
[13] E. A. Williams, B. I. Cohen, L. Divol, M. R. Dorr, J. A. Hittinger, D. E. Hinkel, A. B. Langdon, R. K. Kirkwood, D. H. Froula, and S. H. Glenzer, Phys. Plasmas **11**, 231 (2004).
[14] O. Yaakobi, L. Caspani, M. Clerici, F. Vidal, and R. Morandotti, Opt. Express **21** (2), 1623 (2013).
[15] G. Klughertz, P.-A. Hervieux, and G. Manfredi, J. Phys. D: Appl. Phys. **47**, 345004 (2014).
[16] A. Kovaleva, Phys. Rev. E **92**, 022909 (2015).
[17] A. Kovaleva, Commun. Nonlinear Sci. Numer. Simul. **30**, 373 (2016).
[18] A. Kovaleva, Phys. D (Amsterdam, Neth.) **361**, 28 (2017).
[19] A. Kovaleva, Philos. Trans. R. Soc., A **375**, 20160213 (2017).
[20] A. Kovaleva, Phys. Rev. E **98**, 012205 (2018).
[21] A. F. Vakakis, O. Gendelman, L. A. Bergman, D. M. McFarland, G. Kerschen, and Y. S. Lee, *Passive Nonlinear Targeted Energy Transfer in Mechanical and Structural Systems* (Springer-Verlag, Berlin, New York, 2008).
[22] J. A. Sanders, F. Verhulst, and J. Murdock, *Averaging Methods in Nonlinear Dynamical Systems*, 2nd ed. (Springer, Berlin, 2007).
[23] N. N. Bogoliubov and Y. A. Mitropolski, *Asymptotic Methods in the Theory of Non-Linear Oscillations* (Gordon and Breach, New York, 1961).
[24] A. Kovaleva and L. I. Manevitch, Phys. Rev. E **88**, 024901 (2013).
[25] L. I. Manevitch, A. Kovaleva, and D. S. Shepelev, Phys. D (Amsterdam, Neth.) **240**, 1 (2011).
[26] M. Johansson, G. Kopidakis, S. Lepri, and S. Aubry, Europhys. Lett. **86**, 10009 (2009).
[27] G. A. Korn and T. M. Korn, *Mathematical Handbook for Scientists and Engineers*, 2nd ed. (Dover Publications, New York, 2000).